Organic & Biomolecular Chemistry

ROYAL SOCIETY OF CHEMISTRY

PAPER

View Article Online
View Journal | View Issue

Check for updates

Cite this: *Org. Biomol. Chem.*, 2023, **21**, 3245

Received 31st October 2022,
Accepted 23rd February 2023

DOI: 10.1039/d2ob01989b

rsc.li/obc

Synthesis and ring-opening metathesis polymerisation of *o*-alkoxy benzothiadiazole paracyclophane-1,9-dienes†

Yurachat Janpatompong, Venukrishnan Komanduri, Raja U. Khan and
Michael L. Turner *

ortho-Diethylhexyloxyphenylene benzothiadiazole paracyclophane-1,9-diene as a mixture of diastereomers was synthesized by a sequential benzyne-induced Stevens rearrangement, oxidation and pyrolysis of a dithia[3.3]paracyclophane. Reaction of these highly strained cyclophanedienes with the second generation Grubbs catalyst showed that they can be ring opened to alternating *cis,trans*-phenylenevinylene polymers. *In situ* NMR experiments showed that one isomer **8a** polymerised to 90% conversion, whereas the other **8b** gave only 9% conversion due to steric hindrance on both faces of the alkene bridges of this isomer. The resulting polymers can be readily isomerized in dilute solution using visible light to the all-*trans* isomer and the optical and electrochemical properties of these polymers were examined by theory and experiment.

Introduction

[2.2]Paracyclophanes contain distorted π-electron systems,[1–5] in which the close proximity of the coplanar benzene rings leads to unique electronic properties that have been utilised in asymmetric catalysis for planar chiral derivatives, chemical sensors and liquid crystals.[6–12] [2.2]Paracyclophanedienes, were first synthesised by Cram and Dewhirst in the 1960s[13] and studies have shown that introducing a double bond into the bridges increases the π-interactions between the coplanar aromatic rings and the angles between the bridgehead carbons.[1,14,15] The aromatic rings in many cyclophanes are not planar and are distorted into boat, chair and twisted conformations, consistent with the highly strained nature of these molecules.[1,16–18] The release of this ring strain by metathesis of one of the bridging alkenes in the [2.2]paracyclophanedienes leads to these molecules being effective monomers for ring opening metathesis polymerisation (ROMP) to give well-defined poly(*p*-phenylenevinylenes) (PPVs).[19–25] Paracyclophanedienes with benzothiadiazole (BT) and 2,5-dialkoxy phenylene rings have been reported by Elacqua and Turner *et al.*[23,26] These asymmetric [2.2]paracyclophane-1,9-dienes with electron rich and electron poor building blocks enable the preparation of donor–acceptor PPVs by ROMP.[23,26,27] The alternation of the donor and acceptor moieties within the polymer backbone reduces the polymer band gap and strongly red shifts the optical properties of the material.[28–33]

To date most [2.2]paracyclophane-1,9-dienes reported are substituted at the 2,5-positions (*para*) of the phenylene rings. Substitution at the 2,3-positions (*ortho*) is little reported.[24,25,34] but this substitution pattern is known to lead to PPVs that show significantly blue-shifted optical properties over the comparable 2,5-isomers. *o*-Dialkoxyphenylene benzothiazole paracyclophane-1,9-dienes are unprecedented and in this contribution we report the preparation of these highly strained compounds and examine the stereospecific ring opening of the alkene bridges by alkene metathesis (Scheme 1).

Results and discussion

The synthesis of [3.3]dithiaparacyclophane **4** was achieved by slow addition of a deoxygenated toluene solution of **2**[35] and **3** to a large volume of deoxygenated ethanol containing KOH (Scheme 2). The slow addition reduced the formation of linear and larger cyclic oligomers and favoured the desired intramolecular cyclisation between **2** and **3**.

The ^{1}H NMR spectrum of dithiacyclophane **4** is shown in Fig. 1. Several distinct regions are apparent corresponding to the structural units of the molecule and it is clear that only one isomer of **4** is isolated in high yield (75%) by column

---

*Organic Materials Innovation Centre (OMIC), Department of Chemistry, The University of Manchester, Oxford Road, Manchester, M13 9PL, UK.
E-mail: michael.turner@manchester.ac.uk*

† Electronic supplementary information (ESI) available. See DOI: https://doi.org/10.1039/d2ob01989b

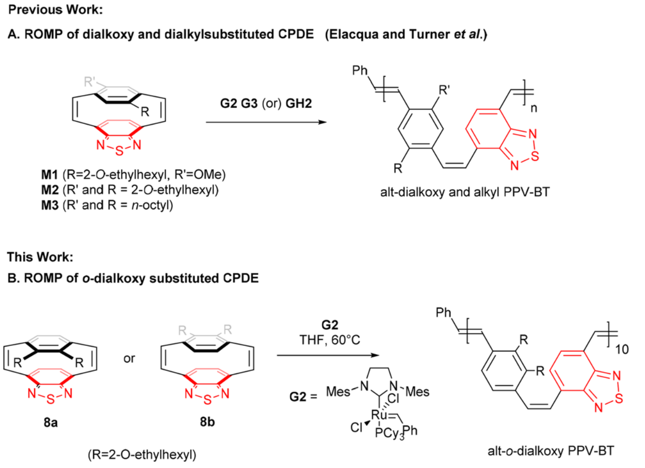

Scheme 1 (A) ROMP approach to *cis*/*trans* D–A dialkoxy and dialkyl D–A PPVBT copolymers.[23,26] (B) ROMP approach to *o*-alkoxy D–A PPVBT copolymer.

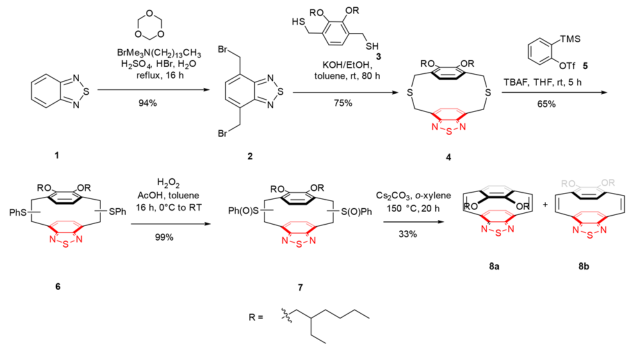

Scheme 2 Synthesis of monomers **8a** and **8b**.

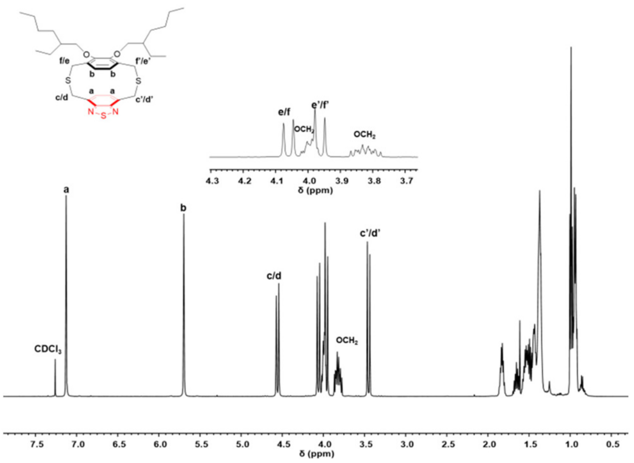

Fig. 1 ^{1}H NMR spectrum of dithia[3.3]paracyclophane **4** in $CDCl_3$.

chromatography. Two singlets, integrating to two hydrogens, at 7.10 ppm (a) and 5.67 ppm (b) were assigned to the four hydrogens of the disubstituted aromatic rings. The doublets at 4.54 and 3.43 ppm integrating to two hydrogens can be assigned to the four thioether hydrogens connected to benzothiadiazole. The other four thioether hydrogens are observed as doublets at 4.04 and 3.94 ppm. The complex multiplets for the OCH_2 hydrogens of the ethylhexyl side chains are observed at 3.98 and 3.80 ppm as shown in the inset of Fig. 1. Based on literature precedence[36] and theoretical calculations (see ESI†), the isomer is assigned as shown in Fig. 1 and Fig. S1.†

A benzyne-induced Stevens rearrangement was performed by the dropwise addition of tetrabutylammonium fluoride trihydrate to a solution of 2-(trimethysilyl)phenyl trifluoromethanesulfonate **5** and **4** in THF at room temperature over a period of 5 hours. After evaporation of the solvent the crude product was purified by flash column chromatography, initially eluting with petroleum ether to remove biphenylene (by-product from the dimerisation of benzyne), followed by elution with 30% DCM/petroleum ether to obtain the mixture of bis-phenyl sulfides **6** as a highly viscous yellow oil in 65% yield. The benzyne-induced Stevens rearrangement is not regioselective and migration of the phenyl sulfide group can occur to either α-carbons (either adjacent to a substituted or unsubstituted ring). Additionally each of these α-carbons is a stereogenic centre and when coupled with the planar chirality this results in a large number of possible isomers of **6**, therefore, the ^{1}H NMR spectrum of compound **6** is very complex with a large number of overlapping signals (see ESI, Fig. S8†). High resolution mass spectrometry (HRMS) gave a molecular ion of 739.2341 *m*/*z* for **6**. This mixture of compounds **6** was then oxidized by addition of hydrogen peroxide (2.2 eq.) in acetic acid and toluene, at room temperature for 20 hours. This gave a complex mixture of compounds **7** as each sulfoxide group is also an additional stereogenic centre (see ESI, Fig. S9†). Thermal elimination of the phenyl sulfoxide groups from compound **7** to generate *cis*-vinylene bonds was achieved by heating to 150 °C in deoxygenated, anhydrous *o*-xylene, under argon for 20 hours. After solvent removal, the crude product was purified by flash column chromatography and an inseparable mixture of the *syn*- and *anti*-cyclophanedienes, **8a** and **8b**, in a ratio of 1 : 3 (by integration of the aromatic protons), was isolated as a reddish oil in a yield of 33%. The ^{1}H NMR spectrum of the cyclophanedienes **8a** and **8b** is shown in Fig. 2.

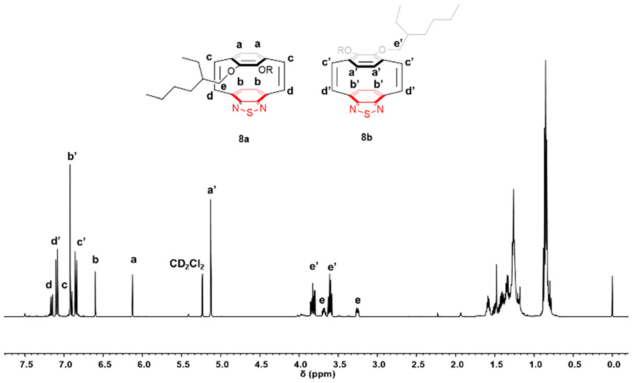

Fig. 2 ^{1}H NMR spectrum of **8a** and **8b** in CD_2Cl_2.

The hydrogens on the benzothiadiazole rings for the two isomers are observed as singlets at 6.60 ppm for **8a** and 6.92 ppm for **8b** in a ratio of 1 : 3. The hydrogens of the phenylene rings appear at 6.13 ppm for **8a** and 5.13 for **8b**, the upfield shift of the hydrogens associated with **8b** is consistent with these hydrogens lying under the thiadiazole ring. The integration of these hydrogens, confirmed the 1 : 3 ratio of the two isomers of **8**. The vinylene hydrogens were observed as two different doublets; at 7.16 ppm and 6.90 ppm with J = 10 Hz in **8a** and 7.09 ppm and 6.85 ppm with J = 10 Hz in **8b**. The protons of OCH_2 group bonded directly to the aromatic ring are diastereotopic and in cyclophanediene **8a** these OCH_2 appear as two multiplets between 3.23–3.27 and 3.65–3.71 ppm. In **8b** these OCH_2 also appear as two multiplets between 3.57–3.64 ppm and 3.78–3.86 ppm. The temperature dependence of the mixture of isomers was studied by ^{1}H NMR spectroscopy (Fig. S15–17†). This showed that the aromatic hydrogens on the phenylene rings ($H_{a'}$) and the *cis*-vinylene bonds ($H_{c'}$) for **8b** appeared as multiplets at temperatures below 293 K. These signals coalesced as the temperature was raised to above 300 K resulting in a sharp singlet and a doublet at the average chemical shift of the multiplets observed at lower temperatures. When the sample was cooled, the original spectrum at room temperature was recovered, consistent with a conformational interconversion. There was no interconversion between isomers **8a** and **8b** observed even at the highest temperatures (325 K).

It was not possible to crystallise either **8a** or **8b** and determine the solid state structure. Hence the ground state geometry of **8a** and **8b** was calculated using density-functional theory calculations (B3LYP/6-311G(d,p)). Both aromatic systems display pseudo-boat conformations. The intramolecular distance between the two carbons of the phenylene group bonded to the vinylene bond is predicted to be 1.5 Å for both **8a** and **8b**. The vinylene bond length in both **8a** and **8b** are calculated to be around 1.35 Å which is in agreement with that of a standard *cis*-vinylene bond 1.32 Å.[37] Each isomer shows a highly strained structure with estimated ring strains of 58 kcal mol^{-1} (**8a**) and 55 kcal mol^{-1} (**8b**). The calculated π–π distances for **8a** and **8b** are very short at 3.06 and 3.04 Å respectively due to the electrostatic attraction between the electron rich and electron poor aromatic rings (Fig. 3).

Initial ROMP studies of monomers **8a** and **8b** with **G2** initiator was conducted using an *in situ* ^{1}H NMR experiment (Fig. 4). Polymerization of monomer **8a** and **8b** was performed in THF-d_8 at 60 °C ([**8a**]/[**G2**] = 10) and ([**8b**]/[**G2**] = 30); after 5 min a signal at δ 16.32 ppm corresponding to the presence of the *O*-chelated carbene intermediate and a signal at δ 17.31 ppm corresponding to the *N*-chelated carbene intermediate were observed but significant quantities of unreacted **G2** remained. After 2 h the initiator was completely consumed and after 24 h the reaction was quenched by adding an excess of ethyl vinyl ether. The crude product was purified by precipitation (MeOH/Celite) followed by elution with chloroform and the desired polymer, **9**, was obtained ($M_{n(calc.)}$ = 5.2 kDa, $M_{n(obs.)}$ = 5.8 kDa, $Đ$ = 1.56). This polymer was derived by the polymerisation of isomer **8a** and **8b**. Specifically, ROMP of isomer **8a** led to 90% conversion, whereas **8b** afforded only 9% conversion (see Fig. S18†). We attribute the higher relative reactivity of **8a** to the presence of an open face of the vinylene bridge (see red arrow) at which the catalyst is able to form the desired metallacyclobutane intermediate by a ring opening methathesis reaction (see Fig. 3c). A similar observation has been seen before in the polymerisation of the tetraalkoxy 2,5-substituted paracyclophanediene derivatives.[17,36] By comparison in compound **8b**, the optimised structure (Fig. 3d) shows steric crowding at both faces of the vinylene bridges by the *o*-alkoxy and benzothiazole groups.

The MALDI-TOF mass spectrum of the 2,3-dialkoxy PPV **9** (Fig. 5) showed a main series of peaks (🟥) separated by an interval of 519 mass units, corresponding to the molecular weight of the monomer. This is consistent with the desired

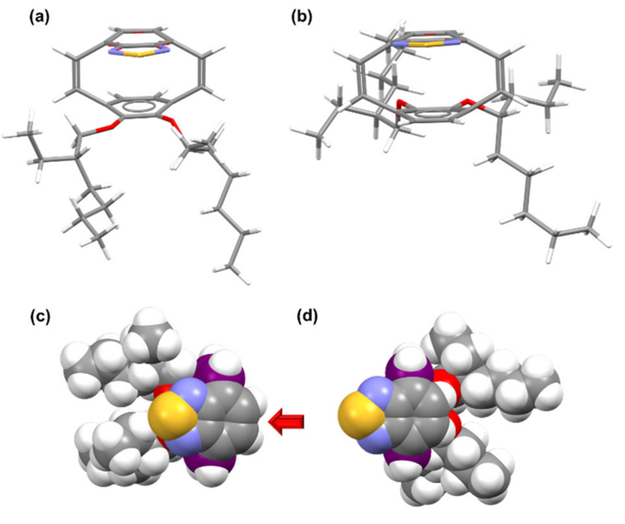

Fig. 3 DFT (Density-Functional Theory) optimized geometry of isomers of **8**: (a and b) Wireframe views of **8a** and **8b**. (c and d) Space-filling views of **8a** and **8b**.

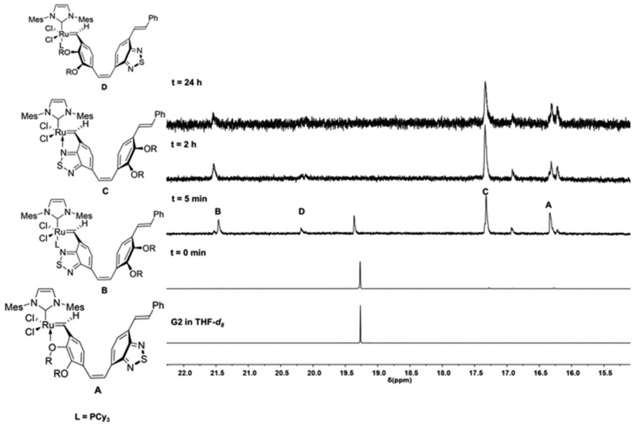

Fig. 4 ROMP of monomer **8a** and **8b** with **G2** catalyst; *in situ* ^{1}H NMR experiment – carbene region.

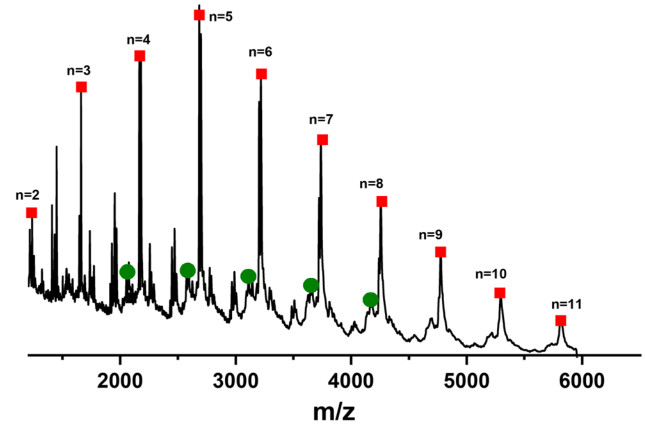

Fig. 5 MALDI-TOF-MS of **9**, (🟥) peaks corresponding to polymers with phenyl and vinyl end groups, and (●) peaks corresponding to cyclic oligomers.

polymer terminated with phenyl and vinyl end groups as expected (total mass 104). A further minor series of peaks (●) was consistent with the formation of cyclic polymers *via* intramolecular secondary metathesis as the active chain end of a propagating polymer can react at the *cis* vinylenes on the same chain, creating a lower molecular weight polymer and a cyclic oligomer. A similar observation has been seen before in the polymerisation of 2,5-dialkoxy PPV polymers.[36]

The ^{1}H NMR spectrum of **9** (Fig. 6) was recorded in $CDCl_3$. The peak at 3.83 ppm can be assigned to the hydrogens of the methylene groups attached to the oxygen for the *cis* and *trans* vinylene links. Signals for the *cis* vinylene groups appear between 6.67 to 7.01 ppm, and those for the *trans* vinylene and other aromatic hydrogens appear further downfield after 7.01 ppm. The copolymer **9** was initially isolated with alternating *cis*/*trans* vinylene stereochemistry. Isomerization to the all *trans* form was achieved by vigorously stirring dilute solutions (1 mg mL^{-1} in dichloromethane) of **9** under exposure to visible light in the absence of oxygen. The *cis* vinylene and phenyl signals can be seen to disappear after isomerisation. In SEC analysis lower retention times were observed for the *trans* isomer relative to their *cis*/*trans* form due to larger hydrodynamic volume of the *trans* isomer (Fig. S23†).

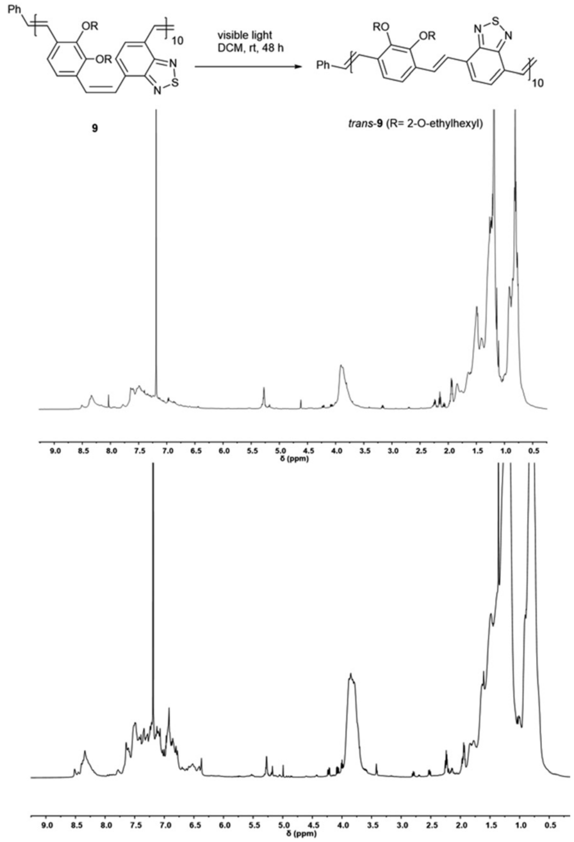

Fig. 6 ^{1}H NMR spectra ($CDCl_3$) of **9** taken before (bottom) and after (top) photoisomerization.

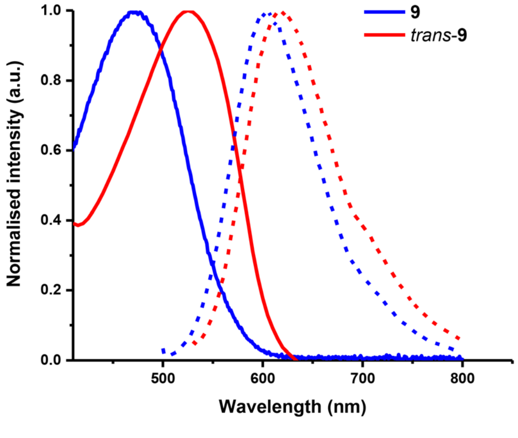

Fig. 7 Absorption and emission profiles of copolymers **9** (Ex = 470 nm) and *trans*-**9** (Ex = 520 nm) in $CHCl_3$ solution.

The absorption and emission spectra of the D–A polymers were recorded in chloroform solution (Fig. 7). The *cis*/*trans* polymer exhibits a λ_{max} of 479 nm, with the PL λ_{max} at 605 nm, the *trans* polymer shows a λ_{max} of 530 nm, with the PL_{max} at 621 nm (see ESI, Fig. S24 and Table S1†). The spectra were red shifted when compared to the analogous 2,3-dialkoxy PPV prepared by the ROMP of a 2,3-dialkoxyparacyclophanediene ($^{abs}\lambda_{max}$ = 384 nm and $^{em}\lambda_{max}$ = 490 nm).[25] They were also red-shifted over the 2,3-dialkoxy PPV polymers reported by Holmes *et al.*, these polymers have two alkoxy groups in the 2,3 position of every phenylene ring, and they exhibited a λ_{max} of 454 nm and a PL_{max} of 519 nm.[34] Incorporation of the BT unit in **9** effectively red-shifts the absorption and emission maximum over the spectra of the reported 2,3-dialkoxy PPV polymers. By comparison the absorption and PL spectra of **9** and *trans*-**9** are blue shifted relative to the optical properties of the 2,5-dialkoxy PPBTV polymers and MEH–PPBTV analogues.[23,26] The blue shift of the absorption maxima can be attributed to the steric interactions of the *ortho*-alkoxy substituents. To investigate this further the ground state structures of oligomers were calculated by DFT using the B3LYP/6-311G(d,p) basis set. The calculations show that oligomers based on **9** and *trans*-**9** are stabilized by intramolecular van der Waals and the electrostatic interactions between heteroatoms.[38] The strong steric repulsions between adjacent sites in the phenylene ring lead to rotation of the substituents around the C(sp^2)–O bonds and consequently hinder effective orbital overlap of the lone pair electrons of the alkoxy-oxygen with the aromatic rings. This causes a more twisted conformation of the polymer backbone (Fig. S2†), which directly affect the λ_{max}.[39]

The electrochemical properties of **9** were investigated using cyclic voltammetry (CV) in an acetonitrile solution of tetrabutylammonium hexafluorophosphate (0.1 M) as electrolyte by drop casting a thin film of **9** on the platinum working electrode. Irreversible oxidation and reductions were observed for *cis*/*trans* **9** and all-*trans* **9** (Fig. S25–27†), against a Ag/$AgNO_3$ reference electrode. The energy levels of the HOMO and the LUMO for the polymers were estimated from the onset of the oxidation and reduction peaks, respectively. The electrochemical bandgap of polymer **9** and *trans*-**9** was observed to be 1.93 eV and 1.87 eV respectively, with the extended conjugation of the *trans*-**9** leading to the smaller band gap, as expected.[20,40]

The nature of the frontier molecular orbitals were examined by DFT calculations using B3LYP/6-311G(d,p) and Fig. 8 shows a plot of the electron density contours of the calculated HOMO and LUMO orbitals. The ethylhexyl side chains of all the structures were replaced with propyl groups to reduce the computational costs without influencing the energy of HOMO and LUMO. For both *cis*/*trans* **9**, and *trans*-**9** the HOMO is delocalized over both the dialkoxyphenylene and the benzothiazole unit while in the case of the LUMO orbital, electrons are predominately localised on the BT acceptor moiety. The energy gaps of the all *trans* structures are lower than alternative *cis*/*trans* conformation in gas phase due to extended conjugation. The calculated HOMO/LUMO energy levels are higher than those obtained from cyclic voltammetry,[41] nonetheless the trends are consistent with the observed experimental data with a reduction around 0.3 eV expected on isomerisation from *cis*/*trans* to *trans* isomers.

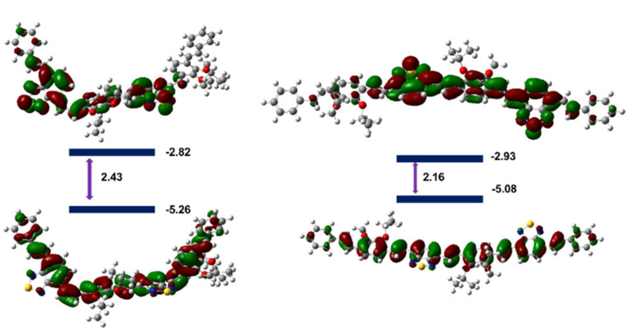

Fig. 8 Calculated HOMO/LUMO energy levels of of *cis*/*trans* **9** and all *trans* **9**.

Conclusions

o-Dialkoxy benzothiadiazole [2.2]paracyclophane-1,9-dienes, **8**, can be synthesised from a [3.3]dithiaparacyclophane (**4**). These highly strained molecules are isolated as a mixture of *syn* and *anti* isomers, **8a** and **8b**, that cannot be interconverted but can be ring opened by ruthenium metathesis catalyst (**G2**) to give regularly alternating *cis*/*trans*-PPV-BT copolymers, **9**. However, **8a** reacted substantially faster than **8b**. The initially formed *cis*/*trans* polymer can be photoisomerised to the corresponding all *trans* isomer. The optical properties were studied in solution and HOMO–LUMO energy levels of the polymers determined by cyclic voltammetry and the orbital contributions investigated by DFT calculation. The all *trans* polymer **9** showed a red shifted absorption maximum with a smaller optical and electrochemical band gaps owing to the enhanced molecular orbital overlap.

Conflicts of interest

There are no conflicts to declare.

Acknowledgements

The authors would like to thank the Development and Promotion of Science and Technology Talents Project (DPST), Thailand for funding to Y. J. The authors would like to thank the European Commission for the award of a Marie-Curie International Fellowship (CyclAr) to V. K. and the EPSRC for funding of the NMR spectrometers under grant EP/K039547/1 and Carlo Bawn for technical advice.

References

1 H. Hopf, *Angew. Chem., Int. Ed.*, 2008, **47**, 9808–9812.
2 Y. Morisaki, K. Inoshita, S. Shibata and Y. Chujo, *Polym. J.*, 2015, **47**, 278–281.
3 I. Majerz and T. Dziembowska, *Mol. Divers.*, 2020, **24**, 11–20.
4 M. Hasegawa, K. Kobayakawa, H. Matsuzawa, T. Nishinaga, T. Hirose, K. Sako and Y. Mazaki, *Chem. – Eur. J.*, 2017, **23**, 3267–3271.
5 S. Park, J. H. Heo, J. H. Yun, T. S. Jung, K. Kwak, M. J. Ko, C. H. Cheon, J. Y. Kim, S. H. Im and H. J. Son, *Chem. Sci.*, 2016, **7**, 5517–5522.
6 Z. Hassan, E. Spuling, D. M. Knoll, J. Lahann and S. Bräse, *Chem. Soc. Rev.*, 2018, **47**, 6947–6963.
7 Z. Hassan, E. Spuling, D. M. Knoll and S. Bräse, *Angew. Chem., Int. Ed.*, 2020, **59**, 2156–2170.
8 N. Khan, N. S. Sheikh, A. F. Khan, R. Ludwig, T. Mahmood, W. Rehman, Y. S. S. Al-Faiyz and K. Ayub, *J. Mol. Model.*, 2015, **21**, 148.
9 U. H. F. Bunz, D. Mäker and M. Porz, *Macromol. Rapid Commun.*, 2012, **33**, 886–910.

10 S. Felder, S. Wu, J. Brom, L. Micouin and E. Benedetti, *Chirality*, 2021, **33**, 506–527.

11 M. Gon, R. Sawada, Y. Morisaki and Y. Chujo, *Macromolecules*, 2017, **50**, 1790–1802.

12 K. Mutoh, Y. Nakagawa, A. Sakamoto, Y. Kobayashi and J. Abe, *J. Am. Chem. Soc.*, 2015, **137**, 5674–5677.

13 K. C. Dewhirst and D. J. Cram, *J. Am. Chem. Soc.*, 1958, **80**, 3115–3125.

14 D. J. Cram, R. C. Helgeson, D. Lock and L. A. Singer, *J. Am. Chem. Soc.*, 1966, **88**, 1324–1325.

15 P. K. Gantzel and K. N. Trueblood, *Acta Crystallogr.*, 1965, **18**, 958–968.

16 A. de Meijere, S. I. Kozhushkov, K. Rauch, H. Schill, S. P. Verevkin, M. Kümmerlin, H.-D. Beckhaus, C. Rüchardt and D. S. Yufit, *J. Am. Chem. Soc.*, 2003, **125**, 15110–15113.

17 F. Menk, M. Mondeshki, D. Dudenko, S. Shin, D. Schollmeyer, O. Ceyhun, T.-L. Choi and R. Zentel, *Macromolecules*, 2015, **48**, 7435–7445.

18 B. J. Lidster, D. R. Kumar, A. M. Spring, C.-Y. Yu, M. Helliwell, J. Raftery and M. L. Turner, *Org. Biomol. Chem.*, 2016, **14**, 6079–6087.

19 B. J. Lidster, D. R. Kumar, A. M. Spring, C.-Y. Yu and M. L. Turner, *Polym. Chem.*, 2016, **7**, 5544–5551.

20 C.-Y. Yu, M. Horie, A. M. Spring, K. Tremel and M. L. Turner, *Macromolecules*, 2010, **43**, 222–232.

21 D. R. Kumar, B. J. Lidster, R. W. Adams and M. L. Turner, *Polym. Chem.*, 2017, **8**, 3186–3194.

22 V. Komanduri, D. R. Kumar, D. J. Tate, R. Marcial-Hernandez, B. J. Lidster and M. L. Turner, *Polym. Chem.*, 2019, **10**, 3497–3502.

23 V. Komanduri, D. J. Tate, R. Marcial-Hernandez, D. R. Kumar and M. L. Turner, *Macromolecules*, 2019, **52**, 7137–7144.

24 A. Mann and M. Weck, *ACS Macro Lett.*, 2022, **11**, 1055–1059.

25 Y. Janpatompong, A. M. Spring, V. Komanduri, R. U. Khan and M. L. Turner, *Macromolecules*, 2022, **55**, 10854–10864.

26 E. Elacqua and M. Gregor, *Angew. Chem., Int. Ed.*, 2019, **58**, 9527–9532.

27 V. Komanduri, Y. Janpatompong, R. Marcial-Hernandez, D. J. Tate and M. L. Turner, *Polym. Chem.*, 2021, **12**, 6731–6736.

28 T. Marszalek, M. Li and W. Pisula, *Chem. Commun.*, 2016, **52**, 10938–10947.

29 M. Kim, S. U. Ryu, S. A. Park, K. Choi, T. Kim, D. Chung and T. Park, *Adv. Funct. Mater.*, 2020, **30**, 1904545.

30 K. Xu, H. Sun, T.-P. Ruoko, G. Wang, R. Kroon, N. B. Kolhe, Y. Puttisong, X. Liu, D. Fazzi, K. Shibata, C.-Y. Yang, N. Sun, G. Persson, A. B. Yankovich, E. Olsson, H. Yoshida, W. M. Chen, M. Fahlman, M. Kemerink, S. A. Jenekhe, C. Müller, M. Berggren and S. Fabiano, *Nat. Mater.*, 2020, **19**, 738–744.

31 J. Miao, H. Li, T. Wang, Y. Han, J. Liu and L. Wang, *J. Mater. Chem. A*, 2020, **8**, 20998–21006.

32 J. Rao, L. Yang, X. Li, L. Zhao, S. Wang, H. Tian, J. Ding and L. Wang, *Angew. Chem., Int. Ed.*, 2021, **60**, 9635–9641.

33 K. Klaue, W. Han, P. Liesfeld, F. Berger, Y. Garmshausen and S. Hecht, *J. Am. Chem. Soc.*, 2020, **142**, 11857–11864.

34 B. S. Chuah, F. Cacialli, D. A. dos Santos, N. Feeder, J. E. Davies, S. C. Moratti, A. B. Holmes, R. H. Friend and J. L. Brédas, *Synth. Met.*, 1999, **102**, 935–936.

35 Z. A. Page, Y. Liu, E. Puodziukynaite, T. P. Russell and T. Emrick, *Macromolecules*, 2016, **49**, 2526–2532.

36 C.-Y. Yu, M. Helliwell, J. Raftery and M. L. Turner, *Chem. – Eur. J.*, 2011, **17**, 6991–6997.

37 F. H. Allen, O. Kennard, D. G. Watson, L. Brammer, A. G. Orpen and R. Taylor, *J. Chem. Soc., Perkin Trans. 2*, 1987, S1–S19.

38 A. S. Özen, C. Atilgan and G. Sonmez, *J. Phys. Chem. C*, 2007, **111**, 16362–16371.

39 P. C. Man, J. A. Crayston, M. Halim and I. D. W. Samuel, *Synth. Met.*, 1999, **102**, 1081–1082.

40 F. Wang, F. He, Z. Xie, M. Li, M. Hanif, X. Gu, B. Yang, H. Zhang, P. Lu and Y. Ma, *J. Polym. Sci., Part A: Polym. Chem.*, 2008, **46**, 5242–5250.

41 H.-W. Tsai, K.-L. Hsueh, M.-H. Chen and C.-W. Hong, *Crystals*, 2021, **11**, 1292.